The International Journal of Advanced Manufacturing Technology (2021) 115:49–59
https://doi.org/10.1007/s00170-021-07218-9

CRITICAL REVIEW

A brief review on welding of stainless steel clad plates: issues and future perspectives

Min Zhu[1] · Wei Wu[2] · Weifang Qian[2] · Liqian Xia[2] · Yansong Zhang[1] · Baosen Wang[2]

Received: 15 December 2020 / Accepted: 3 May 2021 / Published online: 8 May 2021

Abstract
Stainless steel clad plates have been gradually applied in the areas required for both good mechanical properties and corrosion resistance effects, but welding technology is still playing a limiting role in its further large-scale application. The aim of this paper is to review the welding status and future prospective of stainless steel clad plates so as to offer a basis for following research. The paper carefully discussed the welding issues of stainless steel clad plates from three aspects of conventional multi-layer and multi-pass welding, high efficiency welding, and welding finite element simulation, respectively. And simultaneously, the relevant future works were planned too.

Keywords Stainless steel clad plate · Welding · Microstructure · Mechanical properties · Residual stress

1 Introduction

The service environment of metallic structure is becoming more and more complicated as the in-depth advancement of industrialization. Traditional homogenous materials have more problems dealing with the service environment required for corrosion resistance effects. So that, laminated composite materials were designed out to simultaneously meet both mechanical and corrosion resistance requirements for industrial equipment [1, 2]. Stainless steel clad plate (SSCP) is the most common type of binary laminated composite material which always contains 10–20% stainless steel plate except for base carbon plate [3]. Generally speaking, parent base plate is made of low-cost carbon steel such as Q235, Q345, or X65 so as to meet the mechanical property requirements, while parent flyer plate is always single-phase austenitic or duplex stainless steel such as 304, 316L, and 2205 for the sake of corrosion resistance performance. Excellent performance and great cost advantage make the SSCP has already been rapidly promoted in shipbuilding, petrochemical engineering, nuclear power, and automobile manufacturing [4, 5]. It is regarded as one of the most promising types of structural metallic materials in the future.

Due to the great industrial demand, high-efficiency and high-quality preparation technology for SSCP has been developed maturely [6, 7]. In contrast, there are still many problems with its welding and joining procedure. Two component metals with distinct chemical composition, physical and mechanical properties, will lead to microstructural deterioration [8, 9] and excessive internal stress [10] during welding, and hence make the joint properties undesirable. As thus, welding technology has become a major factor restricting the large-scale application of SSCP.

Over the past years, a lot of studies have been done on technological development of SSCP welding. In this paper, the welding status and issues of conventional multi-layer and multi-pass welding, highly efficient welding methods, and the numerical simulation research for SSCP were first reviewed. And meanwhile, the relevant next works were planned.

✉ Yansong Zhang
zhangyansong@sjtu.edu.cn

[1] Shanghai Key Laboratory of Digital Manufacture for Thin-Walled Structures, Shanghai Jiao Tong University, Shanghai 200240, People's Republic of China

[2] Baosteel Research Institute, Baoshan Iron and Steel Co., Ltd., Shanghai 201900, People's Republic of China

2 Conventional multi-layer and multi-pass welding

The dilution between the base plate and flyer plate during welding is the leading cause of microstructural deterioration.

The interdiffusion of main elements in base (C, Fe) and flyer (Cr, Ni) plates may result in hardening region generation on the one hand and corrosion resistance decrease on the other hand [11]. In view of this problem, engineers posted that multi-layer and multi-passes welding should be applied for stainless clad steel plate welding, namely, welding the joint into base, transition, and flyer seam layers.

2.1 Influence of welding sequence

For such type of welding procedure, welding priority of three layers has a great influence on the joint properties. Generally speaking, the welding sequence with base layer first is commonly adopted in most industrial parts manufacturing since it can usually get better joint performance. For instance, Wang et al. [12] welded 2205/16MnR plate with the base layer first and a high-quality joint was obtained with no precipitation of sigma phase (σ) or $M_{23}C_6$. Dhib et al. [13] had prepared the 316L/A283 clad plate joints under three different welding sequences and subsequently compared their mechanical properties. Results were shown in Fig. 1. As we can see, the toughness values of weld metal and heat affected zone (HAZ) in joint under welding sequence with base seam layer welded first were higher than that of the other two joints.

Although other welding sequences always result in deterioration of joint performance, they are inevitable to be adopted in some special cases in engineering, such as the final closure welding of small diameter pipes and pressure tanks in petrochemical industries. In such conditions, single-side welding started from flyer layer is usually adopted. To improve joint performance, engineers always apply stainless steel fillers into all beads welding [14]. For example, Torbati et al. welded 2205 duplex stainless steel clad pipe with flyer plate first by all duplex stainless steel wire metal and a desirable welding joint was obtained under optimized welding methods and parameters [15].

2.2 Influence of the usage of mixed filling metals

The usage of mixed filling metals, namely, applying the stainless steel welding wire for the flyer and transition layer welding and using carbon steel wire for the base layer welding, is very common under the welding sequence started from base layer. And generally, the obtained joints can meet the post-welding test evaluation [12]. But due to the application of mixed filling metals, the multi-layer welding process of stainless clad steel plate essentially belongs to the dissimilar metal welding (DMW) between low carbon steel and stainless steel. Dilution will occur in the local areas near seam layers' interfaces and inevitably result in the generation of martensite phase according to previous study [16]. Li et al. [17, 18] applied the post flyer plate welding process to weld the L415/316L clad plate. Hardness and microstructure characterization showed that about 0.6–0.8-mm-thick hardened martensite layer generated at the interface between stainless and carbon steel seam layers and hence resulted in the crack initiation on the bending test samples although the tensile and bending performance of joints did meet the standards. Similar microstructure

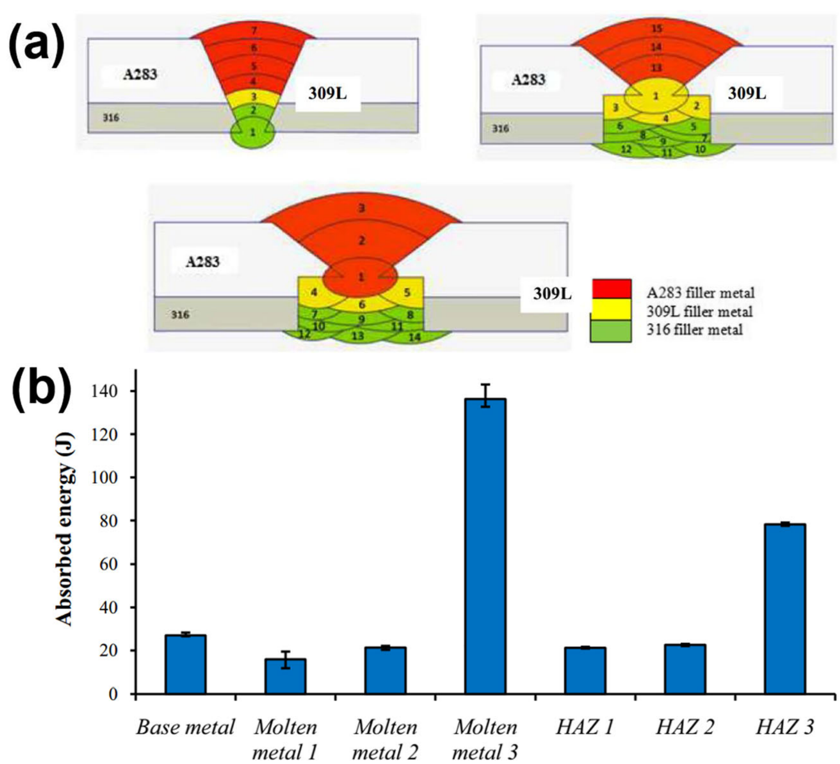

Fig. 1 **a** Passes arrangement schematics of welded joints prepared with different sequences. **b** Measured Charpy V-notch energies [13]

was found in another study too [19]. Although effects of the interfacial martensite layer on the long-term service performance such as fatigue and creep resistance of SSCP joints has not been deeply studied so far, such a thin martensite layer is the common microstructure at interface between stainless and carbon steel DMW joints. From the point of structural integrity, the occurrence of such a hard and brittle layer at interface can obviously cause a lot of problems in subsequent service life of DMW joint [20, 21]. Some targeted controlling methods have already been proposed in DMW, such as inserting buttering layer or using some special groove types [22, 23]. Obviously, these methods are not suitable for interfacial martensite layer controlling in SSCP welding. Extra solutions need to be explored furthermore.

Notably, the local hardening problem due to the usage of mixed filling metals will become more serious under the other welding sequences. For instance, Gou et al. prepared the 2205/X65 bimetallic butt joint according to the welding sequence with flyer layer first. The impact test results showed that impact energy of weld metal (WM) and HAZ of layer 1 (transition and flyer layers) exhibited lower than other two layers, as shown in Fig. 2 [24]. Li et al. [25] welded the 321SS/Q345 bimetallic clad plate with mixed filling metals. Results showed that the martensite formed in the first seam bead filled with carbon steel wires and led to a large area of local hardening zone (LHZ) generated in the WM, as shown in Fig. 3. Although the LHZ had no effect on the tensile properties of the joint, it was still possible to induce crack initiation in the bending test. This kind of joint performance is obviously a hidden risk for safe service of SSCP industrial equipment.

Reported studies demonstrated that the harden martensite phase is bound to generate at the junction of transition layer and the base layer as long as the mixed filling metals were used. And the area of hardened zone would greatly increase under the welding sequence with flyer layer welded first. But the use of mixed filling metals is the inevitable tendency for technological development of SSCP welding since it can greatly reduce the welding cost. So that, improvement solutions need to be found to reduce the amount of hardened microstructure in the future. Some special welding methods may become the viable options. Górnikowska et al. [26] found that the width of the martensite band could be highly limited by using Cold Metal Transfer (CMT) technique for weld overlaying since it introduced low amounts of heat input compared to traditional overlaying methods. Similarly, there are some other feasible welding methods such as TIP Tungsten Inert Gas Arc Welding (TIP TIG) [27], Hot-Wire TIG welding (HW TIG) [28], and Pulsed TIG Welding (P-TIG) [29]. Because all these methods can reduce the arc heat input to the specimen and hence reduce the dilution rate compred to the conventional TIG welding. However, limited comparative studies have been done on the performance between joints prepared by these improved and traditional welding methods.

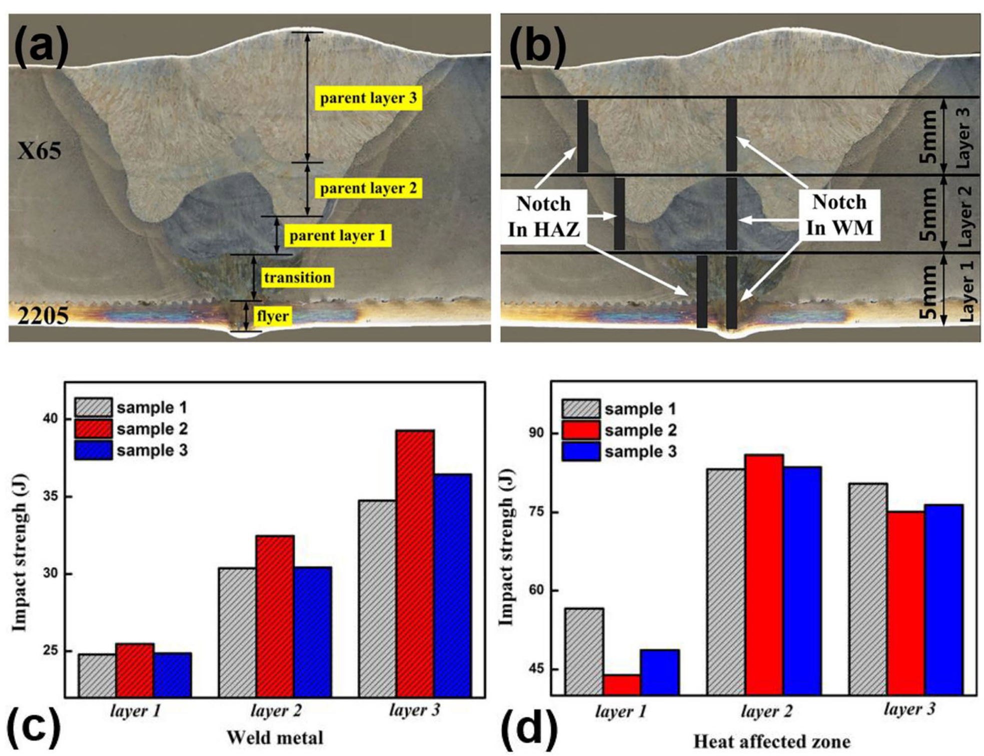

Fig. 2 **a** Morphology of the cross section of the welded joint. **b** Scheme of Charpy impact test. **c** Charpy impact test results for weld metal. **d** Charpy impact test results for HAZ [24]

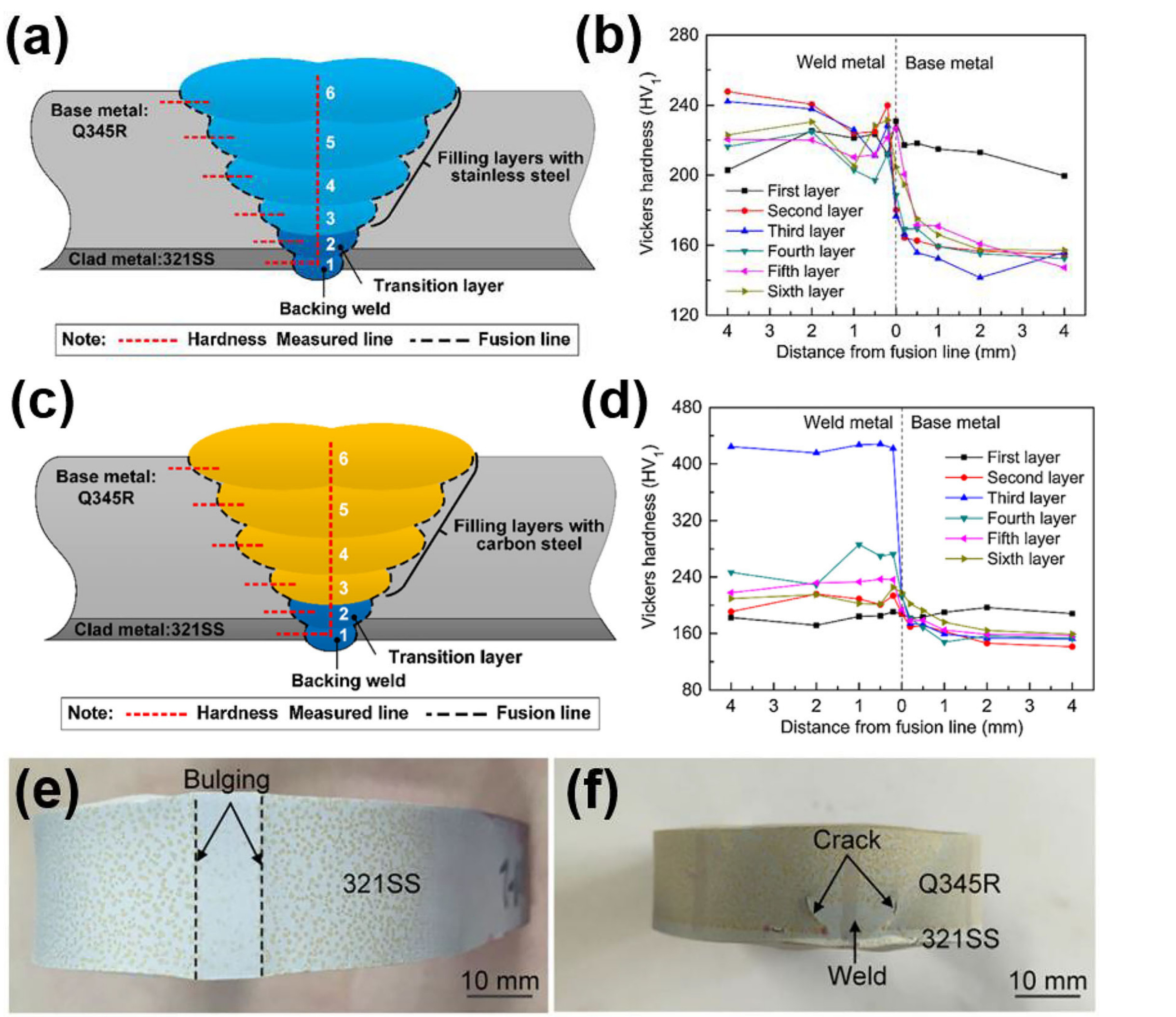

Fig. 3 The welding sequence, microhardness measured lines, and corresponding measured data of joints: **a**, **b** Single metal filled samples. **c**, **d** Mixed metals filled samples. **e** Bulging appear in the face bending test sample of mixed metal filled joints. **f** Cracks appear in the side bending test of mixed metal filled joints [25]

In addition to the generation of hardening zone in the use of mixed welding materials, the multi-layer and multi-pass welding of SSCP still has a fatal drawback, namely, the low welding efficiency. So far, some efforts [30–36] have been done on the high efficiency welding.

3 High efficiency welding

3.1 Laser beam welding

The most direct way to improve welding efficiency of SSCP is to reduce the number of welding passes. Mossori et al. [30] made try to prepare the 304 stainless steel clad plate (2.5 + 6.5mm) by single-pass high-penetration laser beam welding (LBM). The joints obtained showed satisfactory mechanical properties, while Ni-based alloy filler metal was put into the joint in the shape of strips. Similarly, Gou et al. [31] used laser welding to do the single-pass joining of the 2205/X65 SSCP (2 + 2 mm) with the flyer plate set on the bottom side. Results showed that the upper and lower parts of the dumbbell welding seam did show extremely high inhomogeneity on account of the Marangoni convection, as shown in Fig. 4. The high cooling rate of LBM induced the formation of martensite in upper fusion zone (FZ) and hence resulted in the increase of local hardness. Meanwhile, high cooling rate led to the excessive amount of ferrite (unbalanced ferrite/austenite ratio = 65/35) and the second-phase particles within austenite grains in the lower FZ. The undesirable microstructure finally contributed to this area preferentially to fail during the tensile test.

Subsequently, Gou et al. introduced a lagging Metal Inert Gas Welding (MIG) arc (laser-arc distance ≥ 15 mm) so as to counterbalance the excess α-ferrite formed in the lower FZ in

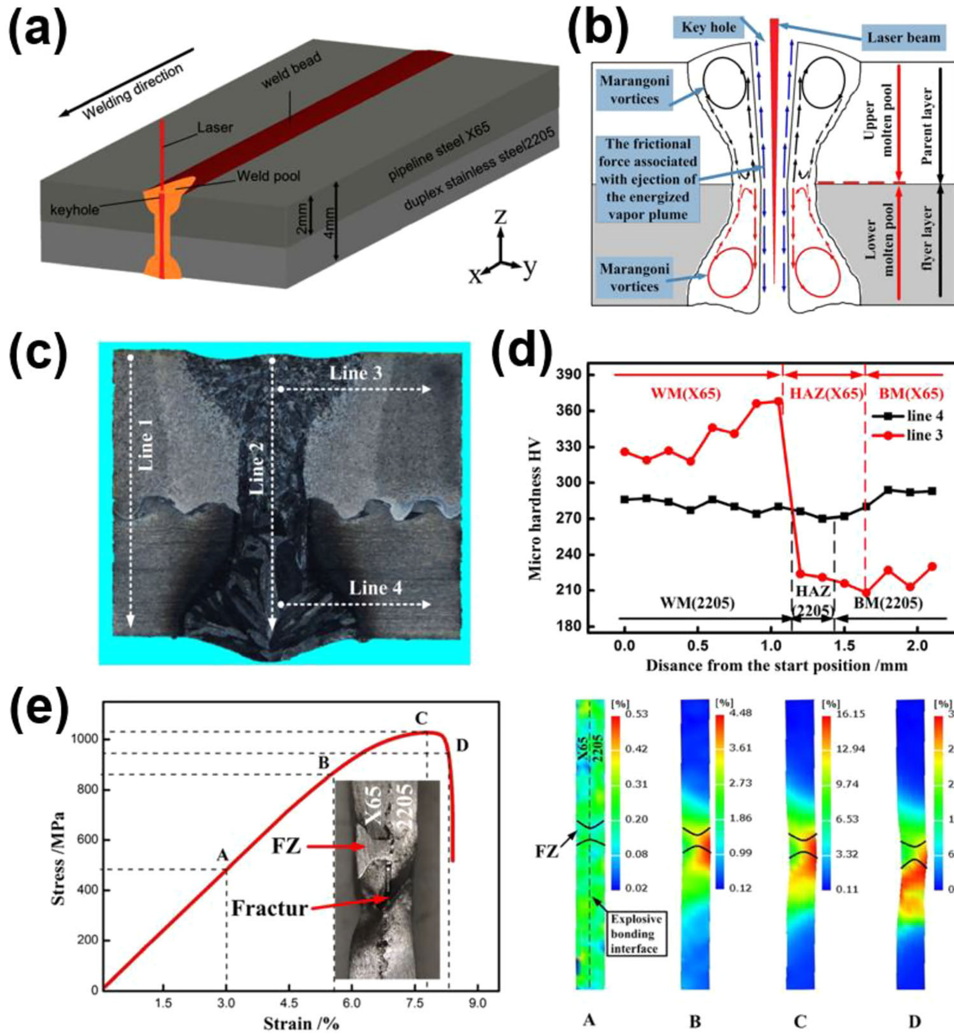

Fig. 4 **a** Schematic sketch of 2205/X65 bimetallic sheet laser butt welding process. **b** Relationship between the flow behavior of the molten pool and the construction of bimetallic sheets. **c** Morphology and the test position of the Vickers hardness test line on the cross section. **d** Results of the microhardness profile along line 3 and 4 on the cross section. **e** Stress-strain curves of the tensile test and the corresponding localized strain distributions on the surface for the same tensile specimen at points A, B, C, and D [31].

the laser beam welding joint, as shown in Fig. 5 [32]. MIG arc heated up the front laser welding seam and allowed a reduction in the cooling rate of laser weld, and hence resulted in more nucleation and growth of austenite in the FZ of flyer layer. But the study pointed out that a desirable joint asked for the extremely strict optimized welding parameters, especially the peak temperature at lower FZ reheated by MIG arc.

3.2 Laser-arc hybrid welding

Laser-arc hybrid welding is one of the high efficiency welding techniques developed rapidly in recent years. It owns many merits such as fast welding speed, deep penetration, and high welding efficiency [33]. Kang et al. [34] applied laser-arc hybrid welding to weld the 304/Q235 SSCP (0.5 + 4.5mm) with different laser-arc distance (D_{LA}). Results showed that tensile properties of joints can be easily ensured under different D_{LA} from 3 to 9 mm, but the corrosion resistance performance strongly depended on the values of D_{LA}. The accepted joint could be obtained with nearly equal corrosion resistance to parent metal by increasing the D_{LA} to 9 mm. The increasing D_{LA} led to the separation of laser and arc heat sources or molten pools and hence reduced the dilution effect of the base layer to increase Cr content and promote the growth of homogeneous cellular grains, as shown in Fig. 6.

Subsequently, Meng et al. [35] studied the influence of type of filling wires imposing on the corrosion resistance of laser-arc welding stainless clad steel joint. Results showed the corrosion resistance property improved as the Cr content increases in the filling wire. Furthermore, Meng et al. [36] found that laser power has greater impact on the weld corrosion resistance compared to wire filling rate.

Studies demonstrate the feasibility of single-pass welding of SSCP by high efficiency welding methods such as laser beam welding and laser-arc hybrid welding, but apparently, the joint performance obtained by reported welding process is

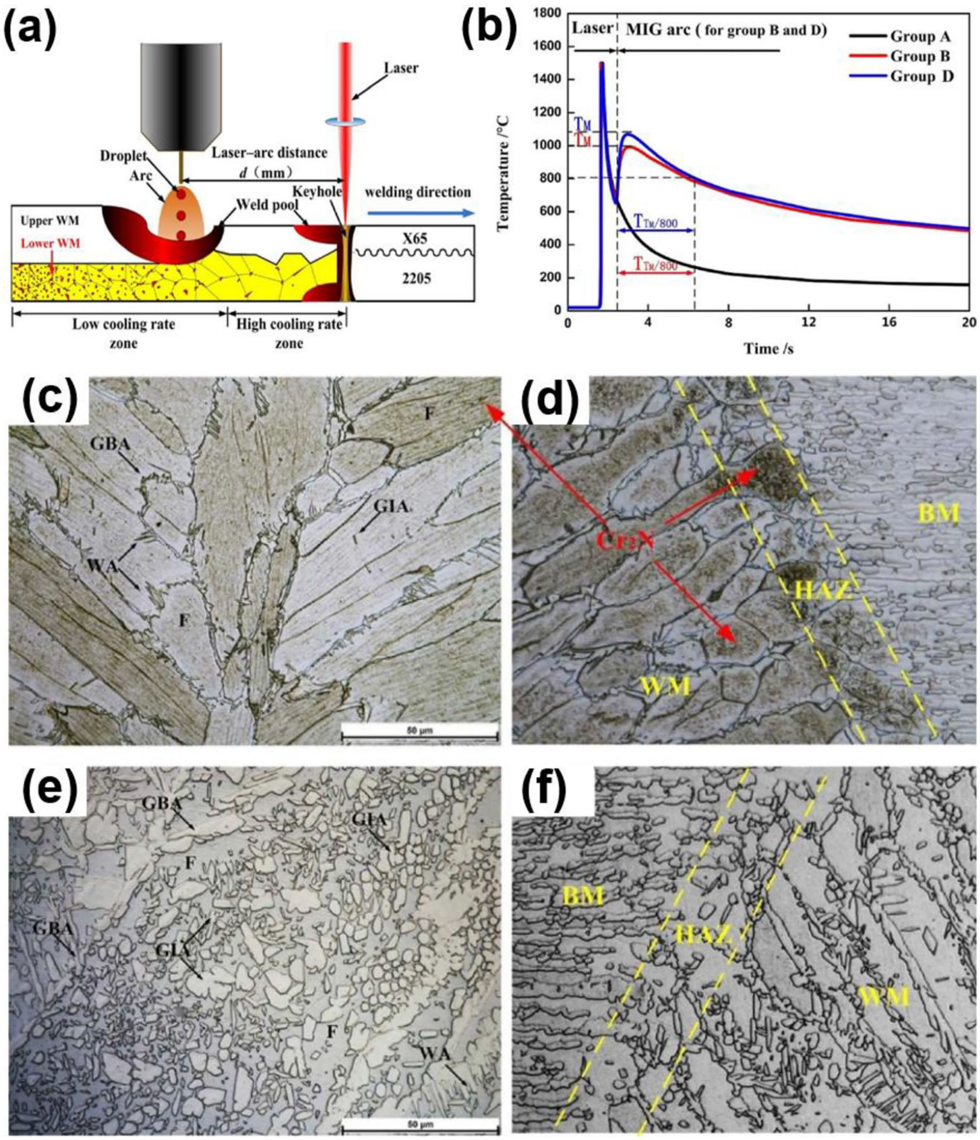

Fig. 5 **a** Schematic sketch of laser-MIG tandem welding process for 2205/X65 bimetallic sheet. **b** Finite element results of thermal histories of lower FZ of laser welding (Group A) and laser-arc hybrid welding (Groups B and D, with 15-mm and 20-mm laser-arc distances, respectively). Microstructures in the FZ: **c** Laser welding samples. **d** Laser-MIG tandem welding samples. Microstructures in HAZ: **e** Laser welding samples. **f** Laser-MIG tandem welding samples [32]

very unstable. More work needs to be done on improving the stability of single-pass welding process. Predictably, the maturity of single-pass welding technology will promote a great revolution of the manufacturing technology of SSCP structures.

3.3 Welding efficiency improvement in multi-pass welding process

Single-pass welding is only applicable for the joining of plates with small thickness (≤9mm). For the medium and thick SSCP, the feasible welding efficiency improvement way is to improve the cladding efficiency of each pass during multi-pass welding. Limited research has been reported in this regard. But Twin-Electrode TIG Welding (T-TIG) welding method may be the workable option [37]. Wu et al. [38, 39] have done lots of investigations on the arc physics and process features of T-TIG. Results found that coupling arc pressure and penetration for T-TIG are lower than single arc (TIG) under the same welding parameters, and meanwhile, the welding speed is much higher. This welding technology is a promising method for high efficiency welding of medium and thick SSCP.

Fig. 6 **a** The experimental set-up. **b** Fracture location of tensile test samples (The D_{LA} of three samples from top to bottom were 3, 6, and 9 mm, respectively). **c** Potentiodynamic polarization curves of samples with different D_{LA}. **d** Effects of D_{LA} on the corrosion potential (E_{corr}), the corrosion current (I_{corr}), the passive potential (E_{pit}), and the passive current density (I_{pit}), obtained by polarization curves. Microstructure of 304SS cladding layer surface of the welds: **e** Nearby fusion line of the weld at D_{LA} 3 mm. **f** FZ centre of the weld at D_{LA} 3 mm. **g** Details of area W3. **h** Nearby fusion line of the weld at D_{LA} 6 mm. **i** FZ centre of the weld at D_{LA} 6 mm. **j** Details of area W6. **k** Nearby fusion line of the weld at D_{LA} 9 mm. **l** FZ centre of the weld at D_{LA} 9 mm. **m** Details of area W9 [34]

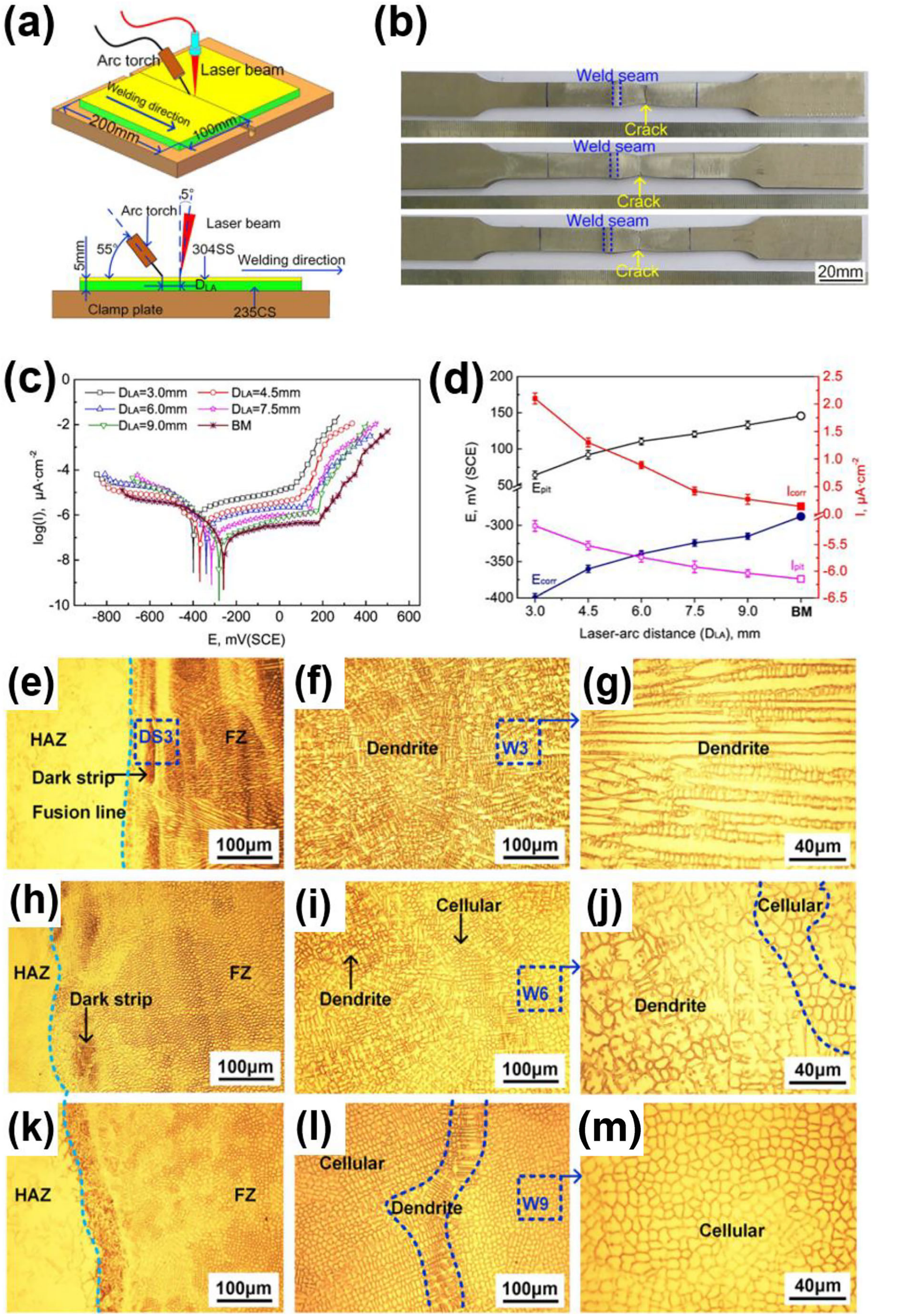
(a)
Arc torch
Laser beam
Welding direction
200mm
100mm
5°
Arc torch
Laser beam
5mm
55°
304SS
Welding direction
DLA
Clamp plate
235CS
(b)
Weld seam
Crack
Weld seam
Crack
Weld seam
Crack
20mm
(c)
DLA=3.0mm
DLA=4.5mm
DLA=6.0mm
DLA=7.5mm
DLA=9.0mm
BM
log(I), μA·cm-2
E, mV(SCE)
(d)
E, mV (SCE)
I, μA·cm-2
Epit
Icorr
Ecorr
Ipit
Laser-arc distance (DLA), mm
(e)
HAZ
DS3
FZ
Dark strip
Fusion line
100μm
(f)
Dendrite
W3
100μm
(g)
Dendrite
40μm
(h)
HAZ
FZ
Dark strip
100μm
(i)
Cellular
Dendrite
W6
100μm
(j)
Cellular
Dendrite
40μm
(k)
HAZ
FZ
100μm
(l)
Cellular
Dendrite
W9
100μm
(m)
Cellular
40μm

4 Numerical simulation of SSCP welding

Besides the improvement of microstructure and mechanical property deterioration, residual stress controlling is also an important aspect of SSCP welding. The magnitude and distribution of residual stresses have a significant impact on structural integrity and stress corrosion cracking resistance of welding joints [10]. Due to the significant differences in physical, mechanical, and metallurgical properties of two component metals, the generation of large amount of residual stress inside SSCP joints is predictable. Because of the difficulty in accurate residual stress measuring by experiment, finite element (FE) method has already become an important approach to welding residual stress prediction. However, there were only few numerical researches reported about welding residual stress of stainless steel clad plates or pipes.

Jiang et al. [40–42] established the sequential-coupled FE models of repair welding process for 304/Q345 clad plates based on Abaqus and studied the influence of several welding factors imposing on the residual stress evolution. They [40] pointed out that large and nonuniform residual stress was generated in the repair welds and the increase of repair weld width could reduce the peak residual stress value, as shown in Fig. 7. In addition, they also found that the heat input and repair welds layer number had great effects on residual stress values. As the heat input and welding layer number increased, the residual stresses decreased [41]. Furthermore, Jiang et al. [42] integrated the FEM with neutron diffraction method so as to get the residual stress distribution feature on the clad plate surface and along the thickness direction of the clad plate joint. Results showed that surficial residual stress was concentrated in the heat affected zone and it was much bigger than the yield strength of 304 stainless steel resulted from the work hardening. And meanwhile, the bending stress would generate in the thickness direction.

In addition, Dong et al. [43] numerically simulated the butt welding of 2205/X65 bimetallic pipe. Its results showed that residual stress around circumferential direction had homogenous distribution except for the welding start/end region. And welding speed has a significant influence on the distribution of inside and outside surficial residual stress. As welding speed decreased, the position of the maximum stress was farther away from the weld centre, as shown in Fig. 8.

It is not hard to find that large amount of welding residual stress will be generated inside the SSCP joint and its peak value and distribution law are strongly influenced by welding parameters. However, there are few studies focusing on the influence of the welding factors during multi-layer and multi-pass welding procedure on the residual stress evolution feature, such as welding sequences, pass arrangements, groove types, and filling metal types. The influence law of these factors on residual stress is very important to the stress prediction and controlling during welding procedure of SSCP. More intensive work should be done in this regard.

5 Conclusion and future work

This paper reviewed the welding status and issues of SSCP from aspects of conventional multi-layer and multi-

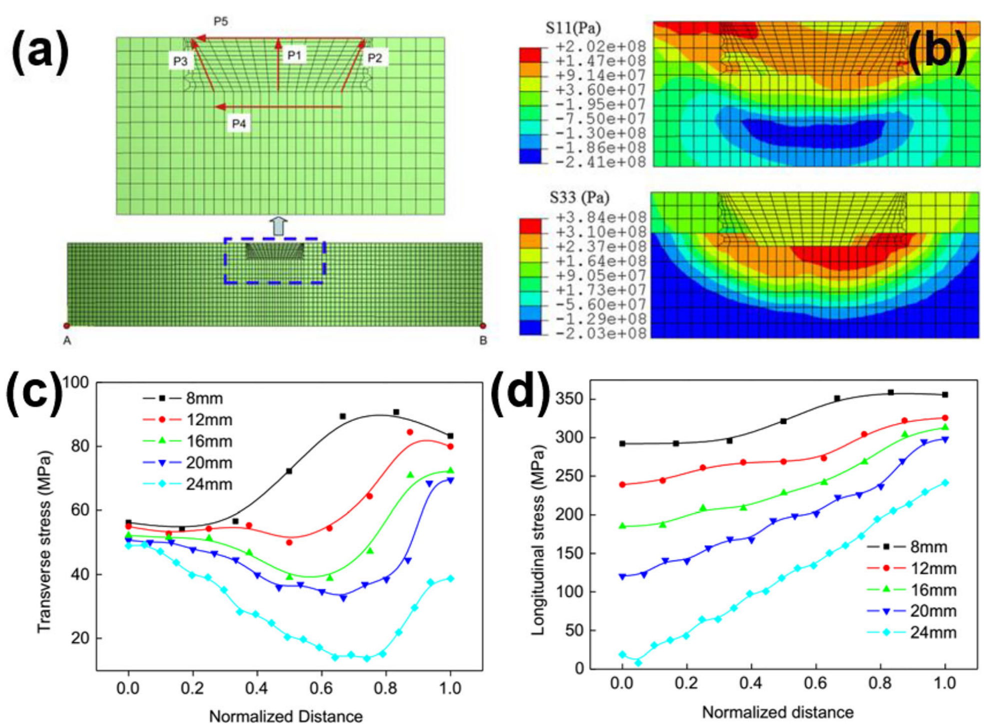

Fig. 7 **a** FE meshing of the repair model (repair weld width = 8 mm). **b** Residual stress contours (transverse stress S11, longitudinal stress S33). **c** Effect of repair width on transverse stress along P4. **d** Effect of repair width on longitudinal stress along P4 [40]

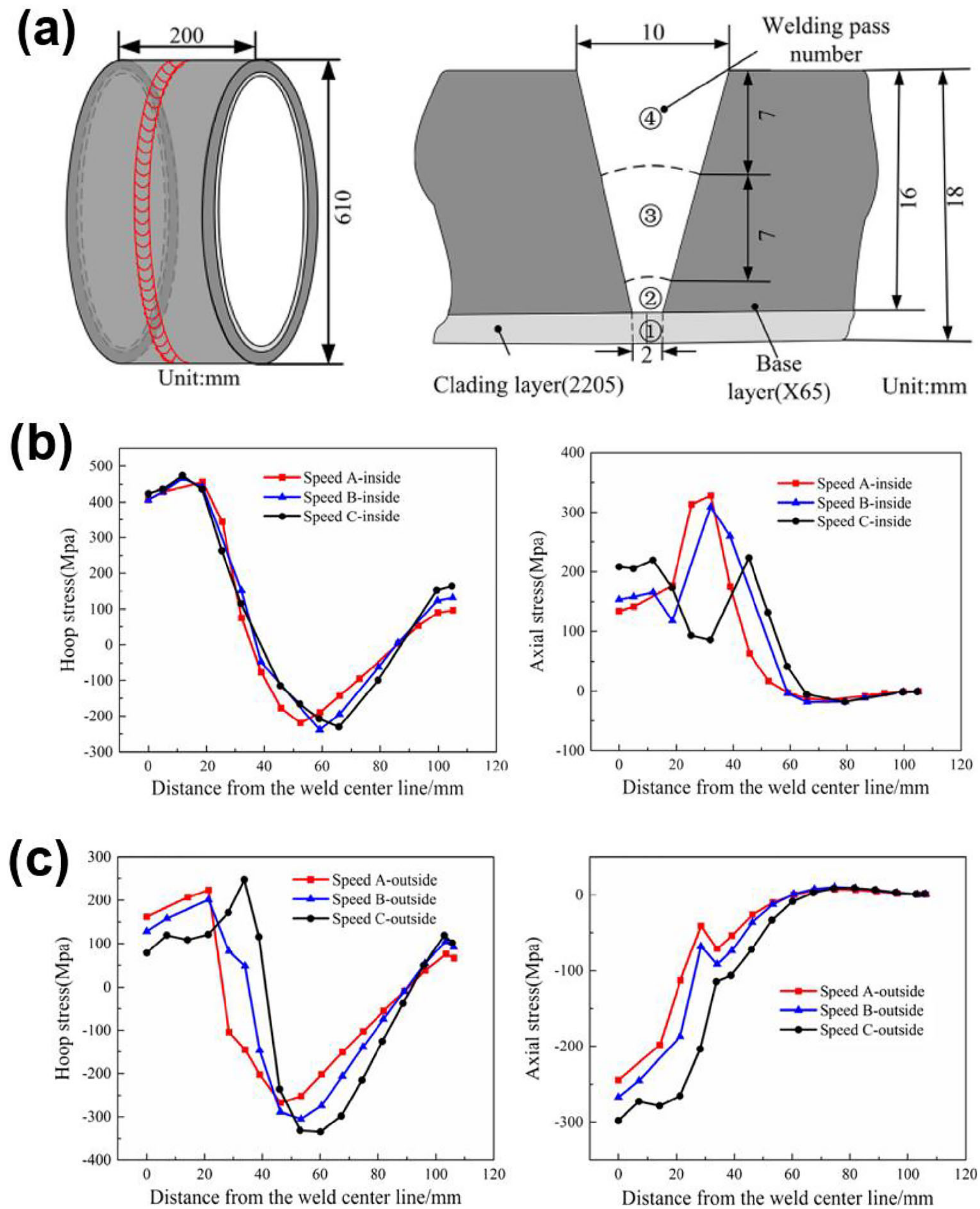

Fig. 8 **a** Dimensions of welded pipe and groove dimension of FE model. **b** Residual stress distribution of hoop and axial stress on the inside surface. **c** Residual stress distribution of hoop and axial stress on the outside surface [43]

pass welding, high efficiency welding, and welding finite element simulation. Based on the reported results, several conclusions can be drawn as follows:

(1) Harden martensite phase was bound to generate at the junction of transition layer and the base layer as long as the mixed filling metals were used in the multi-layer and multi-pass welding.
(2) It is feasible to weld thin SSCP (≤9mm) with single-pass welding by laser beam welding or laser-arc hybrid welding method. But more work needs to be done on improving the stability of single-pass welding process.
(3) Due to the multi-component design, large amount of welding residual stress will be generated inside the SSCP, but few studies focusing on studying the residual stress evolution and controlling of SSCP during welding procedure.

Based on this, we regard that future work can be conducted from the following three aspects:

(1) Improvement solutions suitable for SSCP need to be found which is capable of reducing the amount of hardened microstructure. Some low heat input welding methods may be the feasible options.
(2) Specific methods capable of improving the welding efficiency of medium and thick SSCP still require further studies. Twin-Electrode TIG Welding (T-TIG) method may be the workable way.

(3) The influence of factors during multi-layer and multi-pass welding procedure on the residual stress evolution law, such as welding sequences, passes arrangements, groove types, and filling metal types, can be further explored.

Author contribution Min Zhu: Investigation, Writing. Wei Wu: Conceptualization. Weifang Qian: Conceptualization. Liqian Xia: Conceptualization. Yansong Zhang: Writing, Supervision. Bansen Wang: Conceptualization, Supervision.

Funding This work is supported by the Ministry of Industry and Information Technology of the People's Republic of China (Grant No. MC-201906-Z01).

Availability of data and materials The data sets supporting the results of this paper are included within the paper.

Declarations

Ethical approval Ethics approval was not required for this research.

Consent to participate Not applicable.

Consent for publication The authors do agree that the copyright of this paper is transferred to Springer's journal "The International Journal of Advanced Manufacturing Technology" when the paper is accepted for publication.

Competing interests The authors declare no competing interests.

References

1. Zhang LJ, Pei Q, Zhang JX, Bi ZY, Li PC (2014) Study on the microstructure and mechanical properties of explosive welded 2205/X65 bimetallic sheet. Mater Des 64:462–476
2. Findik F (2011) Recent developments in explosive welding. Mater Des 32:1081–1093
3. Banse J (1998) Newmaterial alternative: stainless and nickel bonded pipes. Stainless Steel World 10:48–49
4. Wu ZJ, Peng WF, Shu XD (2017) Influence of rolling temperature on interface properties of the cross wedge rolling of 42CrMo/Q235 laminated shaft. Int J Adv Manuf Technol 91:517–526
5. Dhib Z, Guermazi N, Ktari A, Gasp M, Hadder N (2017) Mechanical bonding properties and interfacial morphologies of austenitic stainless steel clad plates. Mater Sci Eng A 696:374–386
6. Liu BX, Yin FX, Dai XL, He JN, Fang W, Chen CX, Dong YC (2017) The tensile behaviors and fracture characteristics of stainless steel clad plates with different interfacial status. Mater Sci Eng A 679:172–182
7. Kaya Y, Kahraman N (2013) An investigation into the explosive welding/cladding of Grade A ship steel/AISI 316L austenitic stainless steel. Mater Des 52:367–372
8. Eghlimi A, Shamanian M, Eskandarian M (2015) Evaluation of microstructure and texture across the welded interface of super duplex stainless steel and high strength low alloy steel. Surf Coat Technol 264:150–162
9. Rao NV, Reddy GM, Nagarjuna S (2011) Weld overlay cladding of high strength low alloy steel with austenitic stainless steel—structure and properties. Mater Des 32:2496–2506
10. Jiang W, Fan Z, Li C (2015) Improved steel/aluminum bonding in bimetallic castings by a compound casting process. J Mater Process Technol 226:25–31
11. Rajeev R, Samajdar I, Raman R, Harendranath CS, Kale GB (2001) Origin of hard and soft zone formation during cladding of austenitic/duplex stainless steel on plain carbon steel. Mater Sci Technol 17:1005–1011
12. Wang SG, Dong GP, Ma QH (2009) Welding of duplex stainless steel composite plate: influence on microstructural development. Mater Manuf Process 24:1383–1388
13. Dhib Z, Guermazi N, Gaspérini M, Haddar N (2016) Cladding of low-carbon steel to austenitic stainless steel by hot-roll bonding: microstructure and mechanical properties before and after welding. Mater Sci Eng A 656:130–141
14. SH/T3527-2009 (2012) Specification for welding of stainless clad steel in petrochemical industry. China Petrochemical Press
15. Torbati AM, Miranda RM, Quintino L, Williams S, Yapp D (2011) Optimization procedures for GMAW of bimetal pipes. J Mater Process Technol 211:1112–1116
16. Lippold JC, Kotecki DJ (2005) Welding metallurgy and weldability of stainless steels
17. Li YL, Xiao J, Han B, Wang XL (2020) Microstructure and mechanical properties of welded joints of L415/316L bimetal composite pipe using post internal-welding process. Int J Press Vessel Pip 179:1–10
18. Li YL, Xiao J, Han B, Zhou C, Wang XL (2020) Welding L415/316L bimetal composite pipe using post-internal-welding process. Trans Indian Inst Metals 73:675–689
19. An Q, Fan KY, Ge YF, Liu BX, Liu YC, Wang S, Chen CX, Ji PG, Yin FX (2019) Microstructure and mechanical properties of stainless steel clad plate joints produced by TIG and MAG hybrid welding. J Adhes Sci Technol 34:1–16
20. Rathod DW, Singh RKR, Pandey S, Aravindan S, Singh PK (2017) Influence of graded compositions and carbon diffusivities in buttering on structural integrity of dissimilar metal welds. Mater Sci Eng A 702(15):289–300
21. Wu Q, Xu Q, Jiang Y, Gong JM (2020) Effect of carbon migration on mechanical properties of dissimilar weld joint. Eng Fail Anal 117:1–10
22. Saffari H, Shamanian M, Bahrami A, Szpunar JA (2020) Effects of ERNiCr-3 butter layer on the microstructure and mechanical properties of API 5L X65/AISI304 dissimilar joint. J Manuf Process 50: 305–318
23. Nivas R, Singh PK, Das G, Kumar S, Mahato B, Sivaprasad GM (2017) A comparative study on microstructure and mechanical properties near interface for dissimilar materials during conventional V-groove and narrow gap welding. J Manuf Process 25:274–283
24. Gou NN, Zhang JX, Wang JL, Bi ZY (2017) Butt welding of 2205/X65 bimetallic sheet and study on the inhomogeneity of the properties of the welded joint. J Mater Eng Perform 26:1801–1807
25. Li CA, Qin GL, Tang YS, Zhang BG, Lin SB, Geng PH (2020) Microstructures and mechanical properties of stainless steel clad plate joint with diverse filler metals. J Mater Res Technol 9:2522–2534
26. Rozmus-Górnikowska M, Blicharski M (2017) TEM microstructure and chemical composition of transition zone between steel tube and an Inconel 625 weld overlay coating produced by CMT method. Arch Metall Mater 62:787–793
27. Wang L, Zhao P, Pan J, Tan L, Zhu KX (2021) Investigation on microstructure and mechanical properties of double-sided synchronous TIP TIG arc butt welded duplex stainless steel. Int J Adv Manuf Technol 112:303–312

28. Di XJ, Zhong ZT, Deng CY, Wang DP, Guo XJ (2016) Microstructural evolution of transition zone of clad X70 with duplex stainless steel. Mater Des 95:231–236
29. Eghlimi A, Shamanian M, Raeissi K (2014) Effect of current type on microstructure and corrosion resistance of super duplex stainless steel claddings produced by the gas tungsten arc welding process. Surf Coat Technol 244:45–51
30. Missori S, Murdolo F, Sili A (2004) Single-pass laser beam welding of clad steel plate. Weld J 83:65–71
31. Gou NN, Zhang JX, Zhang LJ, Li ZG, Bi ZY (2016) Single pass fiber laser butt welding of explosively welded 2205/X65 bimetallic sheets and study on the properties of the welded joint. Int J Adv Manuf Technol 86:2539–2549
32. Gou NN, Zhang LJ, Zhang JX (2018) Increased quality and welding efficiency of laser butt welding of 2205/X65 bimetallic sheets with a lagging MIG arc. J Mater Process Technol 251:83–92
33. Moore PL, Howse DS, Wallach ER (2004) Microstructures and properties of laser/arc hybrid welds and autogenous laser welds in pipeline steels. Sci Technol Weld Join 9:314–322
34. Kang K, Kawahito Y, Gao M, Zeng XY (2017) Effects of laser-arc distance on corrosion behavior of single-pass hybrid welded stainless clad steel plate. Mater Des 123:80–88
35. Meng Y, Kang K, Gao M, Zeng XY (2018) Microstructures and properties of single-pass laser-arc hybrid welded stainless clad steel plate. J Manuf Process 36:293–300
36. Meng Y, Kang K, Gao M, Zeng XY (2019) Relationship between corrosion resistance and microstructure characteristic of single-pass laser-arc hybrid welded stainless clad steel plate. Metall Mater Trans A 50:2817–2825
37. Kobayashi K, Nishimura Y, Iijima T, Ushio M, Yanashita M (2004) Practical application of high efficiency twin-arc TIG welding method (Sedar-TIG) for Pclng storage tank. Weld World 48:7–8
38. Zhang GJ, Gao HM, Wu L (2012) Effect of process parameters on temperature distribution in twin-electrode TIG coupling arc. J Quant Spectrosc Radiat Transf 113:1938–1945
39. Leng XS, Zhang GJ, Wu L (2006) Experimental study on improving welding efficiency of twin electrode TIG welding method. Sci Technol Weld Join 11:550–554
40. Jiang WC, Liu Z, Gong JM, Tu ST (2010) Numerical simulation to study the effect of repair width on residual stresses of a stainless steel clad plate. Int J Press Vessel Pip 87:457–463
41. Jiang WC, Wang BY, Gong JM, Tu ST (2011) Finite element analysis of the effect of welding heat input and layer number on residual stress in repair welds for a stainless steel clad plate. Mater Des 32:2851–2857
42. Jiang WC, Woo W, Wang BY, Tu SD (2012) A study of residual stress in the repair weld of stainless steel clad plate by neutron diffraction measurement and finite element method. Acta Metall Sin 48:1525–1529
43. Dong ZQ, Zhang JX (2018) Three-dimensional finite element analysis of residual stresses in circumferential welds of 2205/X65 bimetallic pipe. Int J Adv Manuf Technol 96:2841–2851